DOI: 10.1093/jnci/djq290
Advance Access publication on August 20, 2010.

ARTICLE

Cytosolic Phospholipase A2 and Lysophospholipids in Tumor Angiogenesis

Amanda G. Linkous, Eugenia M. Yazlovitskaya, Dennis E. Hallahan

Manuscript received June 4, 2009; revised August 6, 2009; accepted July 13, 2010.

Correspondence to: Eugenia M. Yazlovitskaya, PhD, Division of Nephrology, Department of Medicine, Vanderbilt University Medical Center, C3210 Medical Center North 1161 21st Ave South, Nashville, TN 37232 (e-mail: eugenia.yazlovitskaya@vanderbilt.edu) and Dennis E. Hallahan, MD, Department of Radiation Oncology, Washington University in St Louis, 4511 Forest Park, St Louis, MO 63130 (e-mail: dhallahan@radonc.wustl.edu).

Background Lung cancer and glioblastoma multiforme are highly angiogenic and, despite advances in treatment, remain resistant to therapy. Cytosolic phospholipase A2 ($cPLA_2$) activation contributes to treatment resistance through transduction of prosurvival signals. We investigated $cPLA_2$ as a novel molecular target for antiangiogenesis therapy.

Methods Glioblastoma (GL261) and Lewis lung carcinoma (LLC) heterotopic tumor models were used to study the effects of $cPLA_2$ expression on tumor growth and vascularity in C57/BL6 mice wild type for ($cPLA_2\alpha^{+/+}$) or deficient in ($cPLA_2\alpha^{-/-}$) $cPLA_2\alpha$, the predominant isoform in endothelium (n = 6–7 mice per group). The effect of inhibiting $cPLA_2$ activity on GL261 and LLC tumor growth was studied in mice treated with the chemical $cPLA_2$ inhibitor 4-[2-[5-chloro-1-(diphenylmethyl)-2-methyl-1*H*-indol-3-yl]-ethoxy]benzoic acid (CDIBA). Endothelial cell proliferation and function were evaluated by Ki-67 immunofluorescence and migration assays in primary cultures of murine pulmonary microvascular endothelial cells (MPMEC) isolated from $cPLA_2\alpha^{+/+}$ and $cPLA_2\alpha^{-/-}$ mice. Proliferation, invasive migration, and tubule formation were assayed in mouse vascular endothelial 3B-11 cells treated with CDIBA. Effects of lysophosphatidylcholine, arachidonic acid, and lysophosphatidic acid (lipid mediators of tumorigenesis and angiogenesis) on proliferation and migration were examined in 3B-11 cells and $cPLA_2\alpha^{-/-}$ MPMEC. All statistical tests were two-sided.

Results GL261 tumor progression proceeded normally in $cPLA_2\alpha^{+/+}$ mice, whereas no GL261 tumors formed in $cPLA_2\alpha^{-/-}$ mice. In the LLC tumor model, spontaneous tumor regression was observed in 50% of $cPLA_2\alpha^{-/-}$ mice. Immunohistochemical examination of the remaining tumors from $cPLA_2\alpha^{-/-}$ mice revealed attenuated vascularity ($P \leq .001$) compared with tumors from $cPLA_2\alpha^{+/+}$ mice. Inhibition of $cPLA_2$ activity by CDIBA resulted in a delay in tumor growth (eg, LLC model: average number of days to reach tumor volume of 700 mm^3, CDIBA vs vehicle: 16.8 vs 11.8, difference = 5, 95% confidence interval = 3.6 to 6.4, $P = .04$) and a decrease in tumor size (eg, GL261 model: mean volume on day 21, CDIBA vs vehicle: 40.1 vs 247.4 mm^3, difference = 207.3 mm^3, 95% confidence interval = 20.9 to 293.7 mm^3, $P = .021$). $cPLA_2$ deficiency statistically significantly reduced MPMEC proliferation and invasive migration ($P = .002$ and $P = .004$, respectively). Compared with untreated cells, $cPLA_2\alpha^{-/-}$ MPMEC treated with lysophosphatidylcholine and lysophosphatidic acid displayed increased cell proliferation ($P = .011$) and invasive migration ($P < .001$).

Conclusions In these mouse models of brain and lung cancer, $cPLA_2$ and lysophospholipids have key regulatory roles in tumor angiogenesis. $cPLA_2$ inhibition may be a novel effective antiangiogenic therapy.

J Natl Cancer Inst 2010;102:1398–1412

Local recurrence in lung cancer and glioblastoma multiforme is a persistent problem despite recent advancements in therapeutic regimens that have improved tumor response (1–4). These tumor types are highly angiogenic and resistant to radiation (5,6). Despite aggressive treatment, most patients with unresectable glioblastoma multiforme have a median survival of approximately 1 year (2,7,8). Patients with unresectable non–small cell lung cancer have a similarly poor prognosis (9–12). Additional treatments are therefore needed to provide improved survival benefits for these patients (13).

Understanding how the tumor microenvironment responds to therapeutic intervention is important for developing efficient molecular targeted pharmacological agents (14–16). We have recently demonstrated that activation of cytosolic phospholipase A2 ($cPLA_2$), an enzyme involved in the formation of lipid second messengers, stimulates proliferation of vascular endothelial cells and promotes the formation of a functional tumor vascular network, thereby contributing to cancer progression (17,18). Upon activation, $cPLA_2$ translocates from the cytosol to cell membranes (19,20), where

it specifically cleaves phosphatidylcholine (21–24) to produce the bioactive lipids lysophosphatidylcholine and arachidonic acid (17,18). In addition to these lipids, which are involved in vascular signaling and tumor progression, lysophosphatidic acid is another $cPLA_2$-derived lipid signaling molecule with known tumorigenic and angiogenic properties (25–27). The major pathways of lysophosphatidic acid production depend on $cPLA_2$ activity: 1) lysophospholipids generated by $cPLA_2$ (such as lysophosphatidylcholine) are subsequently converted to lysophosphatidic acid by lysophospholipase D and 2) phosphatidic acid generated by phospholipase D or diacylglycerol kinase is subsequently converted to lysophosphatidic acid by $cPLA_2$ (28,29). Therefore, $cPLA_2$ is involved in regulating the levels of at least three potent lipid mediators of tumorigenesis and angiogenesis: lysophosphatidylcholine, arachidonic acid, and lysophosphatidic acid. The role of arachidonic acid and lysophosphatidic acid in tumorigenesis has been studied extensively. There is a broad literature linking these two lipids, their turnover, and signaling to cancer progression (24,30–32). There has been active discussion (33,34) regarding the use of arachidonic acid and lysophosphatidic acid signaling pathways as molecular targets for controlling cancer, and several companies are developing drugs for this purpose. By contrast, relatively little is known about the role of lysophosphatidylcholine in tumor progression. Recent studies by our laboratory and others (17,18,35) have shown that lysophosphatidylcholine is a lipid-derived second messenger that triggers the downstream activation of both phosphatidylinositol 3-kinase/Akt and mitogen-activated protein kinase/extracellular signal regulated kinase prosurvival signal transduction pathways, resulting in increased cell viability within the tumor vascular endothelium.

To investigate the effects of $cPLA_2$ and $cPLA_2$-dependent lysophosphatidylcholine production, as well as the roles of arachidonic acid and lysophosphatidic acid, on the growth of lung carcinoma and glioblastoma, we used $cPLA_2\alpha^{-/-}$ C57/BL6 mice, which are deficient in $cPLA_2\alpha$, the predominant isoform of $cPLA_2$ in endothelium, to examine the effect of a deficiency in $cPLA_2$ in the host-derived vascular endothelium on tumor maintenance and progression. In addition, we used murine pulmonary microvascular endothelial cells (MPMEC) isolated from from $cPLA_2\alpha^{-/-}$ mice to investigate the effects of lysophosphatidylcholine, lysophosphatidic acid, and arachidonic acid on cell viability and functions. To further inhibit $cPLA_2$ in cell culture models and in wild-type mice, we used a chemical inhibitor of $cPLA_2\alpha$ known as 4-[2-[5-chloro-1-(diphenylmethyl)-2-methyl-1*H*-indol-3-yl]-ethoxy]benzoic acid (CDIBA), which has been shown to substantially attenuate arachidonic acid release and prostaglandin E_2 production in a wide variety of enzymatic and cell-based assays (36).

CONTEXT AND CAVEATS

Prior knowledge

Two highly angiogenic malignancies—lung cancer and glioblastoma multiforme—remain resistant to existing therapies. Activation of cytosolic phospholipase A2 ($cPLA_2$), an enzyme that catalyzes the formation of bioactive lipids involved in tumorigenesis and angiogenesis, contributes to treatment resistance through transduction of prosurvival signals.

Study design

The effects of $cPLA_2$ expression on glioblastoma and lung tumor growth and vascularity were studied in mice wild type ($cPLA_2\alpha^{+/+}$) and deficient ($cPLA_2\alpha^{-/-}$) in $cPLA_2\alpha$ (the predominant isoform of the enzyme) and in mice injected intraperitoneally with the chemical $cPLA_2$ inhibitor CDIBA. Mouse vascular endothelial 3B-11 cells and murine pulmonary microvascular endothelial cells (MPMEC) isolated from $cPLA_2\alpha^{+/+}$ and $cPLA_2\alpha^{-/-}$ mice were used to study cell proliferation and function and the effects of lipid mediators of tumorigenesis and angiogenesis on proliferation and migration.

Contribution

$cPLA_2\alpha^{-/-}$ mice formed fewer tumors compared with $cPLA_2\alpha^{+/+}$ mice. Tumors from $cPLA_2\alpha^{-/-}$ mice displayed attenuated vascularity compared with tumors from $cPLA_2\alpha^{+/+}$ mice. Inhibition of $cPLA_2$ activity by CDIBA in $cPLA_2\alpha^{+/+}$ mice resulted in a delay in tumor growth and a decrease in tumor size. $cPLA_2$ deficiency or inhibition with CDIBA statistically significantly reduced MPMEC proliferation and invasive migration. Compared with untreated cells, $cPLA_2\alpha^{-/-}$ MPMEC treated with lysophosphatidylcholine and lysophosphatidic acid displayed increased cell proliferation and invasive migration.

Implications

$cPLA_2$ inhibition may be a novel effective antiangiogenic therapy in patients with glioblastoma multiforme and lung cancer.

Limitations

The heterotopic mouse models that were used to study the effect of $cPLA_2$ on tumor growth may not accurately reflect the original tumor organ site.

From the Editors

Materials and Methods

Chemicals

CDIBA was synthesized by the Chemical Synthesis Core Facility of Vanderbilt University (97% purity by nuclear magnetic resonance–mass spectrometry). CDIBA was dissolved in dimethyl sulfoxide (DMSO). L-α-Lysophosphatidylcholine and arachidonic acid were purchased from Sigma–Aldrich (St Louis, MO). Lysophosphatidic acid (18 [carbon atoms]:1 [double bond]) was purchased from Avanti Polar Lipids (Alabaster, AL). All lipids were dissolved in 70% ethanol according to the manufacturers' instructions.

Cell Cultures and Treatment

Murine Lewis lung carcinoma (LLC) cells and murine vascular endothelial 3B-11 cells were purchased from American Type Culture Collection (Manassas, VA). Mouse glioblastoma GL261 cells were obtained from Dr Yancie Gillespie (University of Alabama-Birmingham, Birmingham, AL). The identity of each cell line was verified by immunostaining for specific markers. 3B-11, LLC, and GL261 cells were maintained in Dulbecco's modified Eagle medium containing 10% fetal bovine serum and 1% penicillin–streptomycin (Life Technologies, Gaithersburg, MD) at 37°C and in 5% CO_2. Human umbilical vein endothelial cells (HUVEC) were obtained from Cambrex (East Rutherford, NJ) and were maintained in microvascular endothelial cell growth medium-2

(EGM-2-MV; Cambrex). Cells were treated with vehicle (DMSO) or 2 μM CDIBA in the absence or presence of 10 μM lysophosphatidylcholine, 10 μM lysophosphatidic acid, or 10 μM arachidonic acid for the indicated times before each assay. Cells were treated without induction of serum starvation because it introduces variability and additional stress to the endothelial cell culture systems. Therefore, cells were treated in the same medium in which they had been growing for 2–3 days before treatment.

Isolation of MPMEC

Primary cultures of MPMEC were isolated from 1- to 3-month-old $cPLA_2$ wild-type ($cPLA_2\alpha^{+/+}$) or knockout ($cPLA_2\alpha^{-/-}$) C57/BL6 mice (kindly provided by Dr J. V. Bonventre, Renal Unit, Brigham Women's Hospital, Harvard Medical School, Boston, MA). $cPLA_2\alpha^{+/+}$ and $cPLA_2\alpha^{-/-}$ mice (four of each type) were anesthetized with isoflurane. The lung vasculature was perfused via the right ventricle with phosphate-buffered saline and 2 mM EDTA followed by 0.25% trypsin and 2 mM EDTA. The heart and lungs were excised and incubated in a sterile environment at 37°C for 20 minutes. The visceral pleura were removed, and the perfusion was repeated. The resulting cellular suspension was collected and plated onto tissue culture plates coated with 0.2% gelatin in EGM-2-MV containing 5% fetal bovine serum to enrich for endothelial cells. After several weeks of propagation at 37°C, the proportion of endothelial cells in the cultures was evaluated by immunostaining with a rabbit polyclonal antibody against the endothelial cell marker von Willebrand factor (vWF) (1:100 dilution; Dako, Carpinteria, CA). Staining was detected by immunofluorescence with Alexa Fluor 488–conjugated goat anti-rabbit IgG (1:500 dilution; Invitrogen Molecular Probes, Carlsbad, CA) for 1 hour at room temperature, and cultures with endothelial cell purity greater than 95% were used in proliferation and migration experiments. We followed protocols approved by the Institutional Animal Care and Use Committee of Vanderbilt University when handling and treating all mice used in this study (approved protocol M/04/013).

Matrigel-Based Tubule Formation Assay

The ability of 3B-11 and HUVEC to form capillary-like tubules was analyzed in 24-well plates coated with Matrigel (300 μL per well; BD Biosciences, Bedford, MA) for 30 minutes at 37°C. 3B-11 or HUVEC (10 000 cells per well) were plated onto solidified Matrigel, which simulates the basement membrane matrix, and allowed to attach for 30 minutes before treatment with vehicle (control) or 2 μM CDIBA. The wells were periodically monitored for tubule formation by light microscopy. Tubules formed in control cells at 6 (3B-11) and 24 (HUVEC) hours after treatment. Following tubule formation, digital micrographs of all wells were obtained using an inverted light microscope at ×20 and ×40 magnification. Tubules from four randomly selected ×40 high-power fields (HPFs) per sample were counted, and results are presented as the average number of tubules per HPF. Samples were assayed in triplicate from three independent experiments.

Scratch Assay for Cell Migration

3B-11 or LLC cells were grown to 70%–80% confluency in 60 × 15 mm cell culture dishes. Four parallel wounds were created on each plate by scratching the cell monolayer with a 10-μL pipette tip, and boundaries of the wounds were marked. Cells were treated for 24 hours with vehicle or 2 μM CDIBA. The cells were then stained with 1% methylene blue, and cells found inside and outside of the wound boundaries were counted from six HPFs per sample. Cells that spanned the boundaries were classified as non-migrated cells. Cell density within the wound is presented as a percentage of total cell density in the plate. Results are from triplicate samples in three independent scratch assays.

Boyden Chamber Transwell Invasion and Migration Assay

3B-11 (50 000 cells per well) or MPMEC (80 000 cells per well) were added to the top chamber of 24-well plates containing Matrigel-coated transwell insert filters (8-μm pore size; Costar Corning, Corning, NY). Fresh medium (600 μL) was added to the bottom chamber, and the cells were incubated for 30 minutes to allow attachment to the inserts. Both chambers were then treated with vehicle or 2 μM CDIBA (3B-11 cells only) in the absence or presence of 10 μM lysophosphatidylcholine, 10 μM lysophosphatidic acid, or 10 μM arachidonic acid. The cells were incubated for 24 hours at 37°C in 5% CO_2. All cells on the upper surface of the transwell insert filter were removed with a cotton swab. The insert filters were rinsed in phosphate-buffered saline, fixed in 100% methanol, and stained with 4′,6-diamidino-2-phenylindole (DAPI; 2.5 ng/μL). Cells that had migrated through the filter (ie, those on the lower surface of the filter) were photographed with the use of a Zeiss fluorescent microscope and counted for four randomly selected HPFs from each sample. The average number of migrated cells per HPF was calculated for three independent experiments.

Cell Proliferation Assays

Ki-67 Immunofluorescence Staining. 3B-11, MPMEC, or LLC cells were grown to 60%–70% confluency on slides. Cultures were treated with vehicle or 2 μM CDIBA (3B-11 and LLC cells only) for 24 hours in the absence or presence of 10 μM lysophosphatidylcholine, 10 μM lysophosphatidic acid, or 10 μM arachidonic acid. The cells were fixed in ice-cold methanol and permeabilized in 0.25% Triton X-100 for 10 minutes at room temperature. Following permeabilization, the cells were incubated overnight at 4°C with a rabbit polyclonal antibody against Ki-67 (1:100 dilution; Abcam, Inc, Cambridge, MA) followed by incubation with Alexa Fluor 488–conjugated goat anti-rabbit IgG (1:500 dilution; Invitrogen Molecular Probes) for 1 hour at room temperature. The cells were counterstained with DAPI (2.5 ng/μL), and Ki-67–positive cells were detected by immunofluorescence microscopy and counted in four randomly selected HPFs per sample. Positive cells were classified as those in which nuclear fluorescence was present, and KI-67–negative cells were those in which no nuclear fluorescence was detected. Samples were analyzed in triplicate from three independent experiments, and Ki-67–positive cells were presented as a percentage of the number of Ki-67–positive cells in vehicle-treated control cells.

5-Bromodeoxyuridine Incorporation. 3B-11 cells were plated in 96-well plates (5000 cells per well) and incubated for 24 hours. The cells were treated with vehicle or 2 μM CDIBA for 24 or 72 hours in the absence or presence of 10 μM lysophosphatidylcholine, 10 μM

lysophosphatidic acid, or 10 μM arachidonic acid. Incorporation of 5-bromodeoxyuridine (BrdU) was measured in each well with the use of an enzyme-linked immunosorbent assay–based 5-Bromo-2′-deoxy-uridine Labeling and Detection Kit III (Roche Applied Science, Indianapolis, IN) according to the manufacturer's instructions. BrdU incorporation was quantified by a change of absorbance (optical density) at 405 nm. Samples were analyzed in triplicate from three independent experiments.

MTS Assay for Metabolic Activity

3B-11 cells were plated in 96-well plates (5000 cells per well) and allowed to attach for 24 hours. Cultures were treated with vehicle or 2 μM CDIBA for 24 or 72 hours in the absence or presence of 10 μM lysophosphatidylcholine, 10 μM lysophosphatidic acid, or 10 μM arachidonic acid. Metabolic activity was analyzed by a form of the 3-(4, 5-dimethylthiazol-2-yl)-5-(3-carboxymethoxyphenyl)-2-(4-sulfophenyl)-2H-tetrazolium, inner salt (MTS) assay using a CellTiter 96 AQ_{ueous} Non-Radioactive Cell Proliferation Assay kit (Promega, Madison, WI) according to the manufacturer's instructions. Metabolic activity was expressed as absorbance (optical density) at 490 nm and was assessed from triplicate samples in three independent experiments.

Mouse Tumor Models, Treatments, and Tumor Growth Delay Studies

We followed protocols approved by the Institutional Animal Care and Use Committee of Vanderbilt University when handling and treating all mice used in this study (approved protocols M/04/013 and M/07/358).

We used C57/BL6 $cPLA_2\alpha^{+/+}$ and $cPLA_2\alpha^{-/-}$ mice (provided by Dr J. V. Bonventre). The $cPLA_2\alpha^{-/-}$ mouse was created by disruption of an exon containing Ser228, which is critical for $cPLA_2\alpha$ catalytic activity, in mouse embryonic stem cells (37). The homozygous null mice experience normal development, weight gain, and life spans and do not exhibit any spontaneous tumor formation. As expected, $cPLA_2\alpha^{-/-}$ mice have reduced levels of eicosanoid production (37).

For tumor growth studies in $cPLA_2\alpha$-deficient mice, LLC (10^6) or GL261 (2×10^6) cells were injected subcutaneously into the right hind limbs of $cPLA_2\alpha^{+/+}$ and $cPLA_2\alpha^{-/-}$ mice (n = 6–7 mice per group). The volumes of the resulting tumors were measured at 48-hour intervals using power Doppler sonography as described below.

For tumor growth delay studies in mice treated with CDIBA, LLC (10^6) or GL261 (2×10^6) cells were implanted into the right hind limbs of $cPLA_2\alpha^{+/+}$ C57/BL6 mice. Once, all tumors exceeded 2 mm in diameter (approximately 2 weeks later), as determined by external caliper measurements, the mice were stratified into groups of six to seven animals representing similar distributions of tumor sizes (range = 3–5 mm in diameter). LLC tumor–bearing mice were injected intraperitoneally with vehicle (DMSO) or CDIBA at 0.5 or 1.0 mg per kg body weight once daily for five consecutive days. GL261 tumor–bearing mice were treated with vehicle or CDIBA at 1.0 mg per kg body weight once daily for seven consecutive days. Tumor size was monitored by external caliper measurements at 48-hour intervals. Mice were killed by cervical dislocation once tumors reached a volume of approximately 700 mm^3 or exceeded 15 mm in diameter, per Animal Care guidelines.

Power Doppler Sonography

Tumors were sonographically imaged with a VEVO 770 small-animal high-resolution ultrasound scanner equipped with a 40-MHz transducer and a mechanically scanned single-element aperture (VisualSonics, Toronto, ON, Canada). The focal zone of the transducer was set at 6 mm from the scanning surface. The scanning plane was perpendicular to the long axis of the lower extremity along the entire length of the tumor. Three-dimensional images in power Doppler mode were obtained by computer-controlled translation of the transducer over the whole length of the tumor by acquiring two-dimensional images every 100 μm. The following ultrasound scanner settings were used: a power Doppler transmission frequency of 23 MHz, a power gain of 100%, a wall filter of 2.3 mm/s, and a scan speed of 2.0 mm/s. Three-dimensional tumor volume was reconstructed by using semiautomated segmentation of 10–12 parallel planes through the two-dimensional images with the use of VisualSonics image analysis software.

Assessment of $cPLA_2$ Activity and Lysophosphatidic Acid Concentration in Plasma From Tumor-Bearing Mice

Vehicle or CDIBA at 1.0 mg per kg body weight was intraperitoneally injected once daily for five consecutive days into LLC tumor–bearing $cPLA_2\alpha^{+/+}$ mice (five mice per group). Mice were anesthetized with ketamine/xylazine, and blood samples were collected from the tail veins immediately before the initiation of treatment and 1 hour after the final treatment. Blood samples were immediately processed for plasma isolation and stored at −80°C. $cPLA_2$ activity in thawed plasma samples was analyzed by using a $cPLA_2$ activity kit (Cayman Chemical, Ann Arbor, MI) according to the manufacturer's instructions. Briefly, thawed plasma samples were incubated with 1.5 mM arachidonoyl thio-phosphotidylcholine (a $cPLA_2$ substrate) for 1 hour at room temperature. Enzyme catalysis was stopped by the addition of beta dystrobrevin/EGTA, and the optical density of the sample was measured at 405 nm. $cPLA_2$ activity was expressed in micromoles per minute per milliliter. Lysophosphatidic acid concentration was assessed by a competitive enzyme-linked immunosorbent assay (Echelon Biosciences, Inc, Salt Lake City, UT) according to the manufacturer's instructions and was expressed in micromoles.

Histological Analysis of Tumor Vascularity

In the tumor growth delay studies, once LLC tumors from $cPLA_2\alpha^{+/+}$ and $cPLA_2\alpha^{-/-}$ mice reached a volume of approximately 700 mm^3, the mice were killed by cervical dislocation and the tumors were resected, fixed in 10% formalin, and sectioned. Sections (5 μm thick) underwent antigen retrieval by pretreatment with 20 μg/mL proteinase K for 30 minutes at room temperature and then were incubated with a rabbit polyclonal antibody against human vWF (1:100 dilution; Dako). Sections were subsequently incubated with Alexa Fluor 488–conjugated goat anti-rabbit IgG (1:500 dilution; Invitrogen Molecular Probes) for 1 hour at room temperature. Sections were studied by immunofluorescence microscopy, and the Alexa Fluor 488–stained vessels were counted in six randomly selected HPFs per sample. Vascularity was determined as the average number of stained vessels per HPF. Tissue integrity was assessed by standard hematoxylin–eosin staining and microscopy.

Co-staining of Mouse Tumors for vWF and Alpha-Smooth Muscle Actin or Desmin

Slides containing formalin-fixed LLC tumor sections (5 μm thick) were incubated with 20 μg/mL proteinase K as described above, followed by incubation for 1 hour at room temperature with the mouse immunoglobulin blocking reagent from a M.O.M. Immunodetection Kit (Vector Laboratories, Burlingame, CA). Sections were then incubated at 4°C overnight with rabbit polyclonal anti-human vWF antibody and either a monoclonal mouse anti-human α-smooth muscle actin (α-SMA) antibody or a monoclonal mouse anti-human desmin antibody (all at 1:100 dilution; Dako). The slides were rinsed in phosphate-buffered saline, and the sections were incubated with DAPI (1:1000 dilution), Alexa Fluor 594–conjugated goat anti-mouse IgG (1:200 dilution; Invitrogen Molecular Probes), and Alexa Fluor 488–conjugated goat anti-rabbit IgG (1:500 dilution; Invitrogen Molecular Probes) for 1 hour at room temperature. Positive staining was determined by immunofluorescence microscopy.

Statistical Analysis

The Student *t* test or the Mann–Whitney rank sum test was used to compare two groups and one-way analysis of variance and Holm–Sidak multiple-group posttest comparisons was used for comparisons among multiple groups. All statistical tests were two-sided, and the statistical analysis was done with the use of SigmaStat software (Systat Software, Inc, San Jose, CA). Longitudinal analysis was performed on serial tumor volume data. Statistical significance was defined as P less than .05. Data are presented as mean values with 95% confidence intervals (CIs).

Results

Effect of Lysophospholipids on Proliferation of $cPLA_2$-Deficient and CDIBA-Treated Mouse Vascular Endothelial Cells

Because new blood vessel formation requires vascular endothelial cell proliferation, we used primary MPMEC isolated from $cPLA_2\alpha^{+/+}$ or $cPLA_2\alpha^{-/-}$ mice to assess the effects of $cPLA_2$ deficiency on cell growth and proliferation. MPMEC were first stained with an antibody to Ki-67, an established cell proliferation marker. Ki-67 staining in $cPLA_2\alpha^{-/-}$ cells was reduced to 41.4% (95% CI = 16.5% to 66.3%, P = .002) compared with $cPLA_2\alpha^{+/+}$ cells (Figure 1, A). Further evidence that $cPLA_2$ supports endothelial cell proliferation resulted from Ki-67 immunostaining of LLC lung tumor cells and vascular endothelial 3B-11 cells that were treated with the $cPLA_2$ inhibitor, CDIBA (2 μM), or vehicle. The number of Ki-67–positive 3B-11 cells treated with CDIBA was reduced to 43.8% (95% CI = 27.0% to 60.6%, P < .001) compared

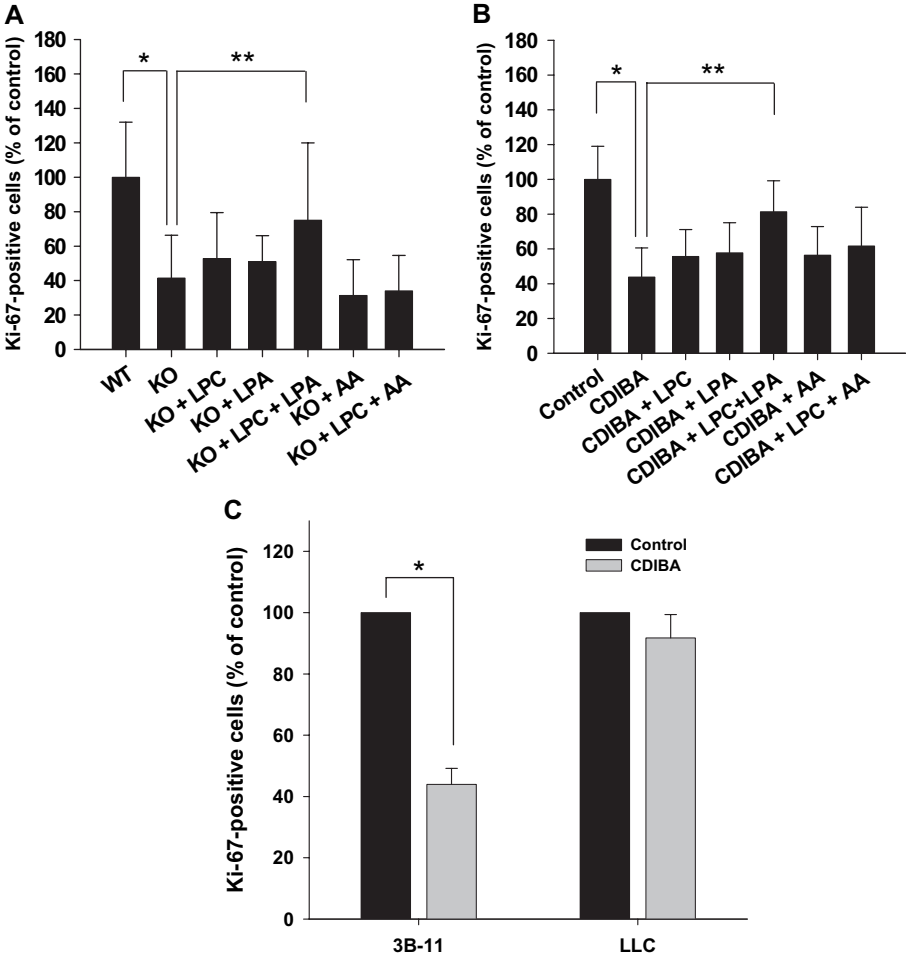

Figure 1. Effect of lysophospholipids on proliferation of $cPLA_2$-deficient and CDIBA-treated vascular endothelial cells. $cPLA_2\alpha^{+/+}$ (wild-type [WT]) and $cPLA_2\alpha^{-/-}$ (knockout [KO]) murine pulmonary microvascular endothelial cells (**A**), murine vascular endothelial 3B-11 cells (**B**,**C**), or Lewis lung carcinoma (LLC) cells (**C**) were grown to 60%–70% confluency. Cultures were treated with vehicle (control) or 2 μM CDIBA (3B-11 and LLC only) in the absence or presence of 10 μM lysophosphatidylcholine (LPC), 10 μM lysophosphatidic acid (LPA), or 10 μM arachidonic acid (AA) for 24 hours. Proliferation was assayed by staining the cells with an antibody against Ki-67 and immunofluorescence microscopy. The number of Ki-67–positive cells was counted in four randomly selected high-power microscopic fields from each sample in triplicate and is expressed as the mean percentage of the number of Ki-67–positive cells in the control sample in three independent experiments; **error bars** correspond to 95% confidence intervals. **A**): **P* = .002 (Student *t* test); ***P* = .011 (analysis of variance [ANOVA]). **B**): **P* < .001 (Mann–Whitney rank sum test); ***P* = .001 (ANOVA). **C**): **P* = .004 (Student *t* test). All *P* values are two-sided.

with 3B-11 cells treated with vehicle alone (Figure 1, B). By contrast, inhibition of $cPLA_2$ by CDIBA had no statistically significant effect on the percentage of Ki-67–positive LLC tumor cells compared with LLC cells treated with vehicle alone (91.8% [CDIBA] vs 100% [vehicle], difference = 8.2%, 95% CI = −6.6% to 23.2%, $P = .464$) (Figure 1, C).

By using a more direct assay of cellular proliferation, we found that BrdU incorporation was reduced by 50% (95% CI = 15.4% to 85.6%, $P = .03$) in 3B-11 cells treated with CDIBA compared with control cells treated with vehicle alone (data not shown). Conversely, an MTS assay for metabolic activity revealed no statistically significant difference between CDIBA-treated 3B-11 cells and 3B-11 cells treated with vehicle alone (data not shown), suggesting that $cPLA_2$ inhibition affects the proliferative status but not the metabolic processes of vascular endothelial cells.

$cPLA_2$ is essential for the production of three bioactive lipid mediators: arachidonic acid, lysophosphatidylcholine, and lysophosphatidic acid (24,27). To examine whether any of these three lipids contribute to vascular endothelial cell proliferation, we incubated MPMEC from $cPLA_2\alpha^{-/-}$ and CDIBA-treated 3B-11 cells with 10 μM lysophosphatidylcholine, 10 μM lysophosphatidic acid, or 10 μM arachidonic acid for 24 hours and then assessed the cells for Ki-67 staining. Compared with untreated $cPLA_2\alpha^{-/-}$ MPMEC, treatment of $cPLA_2\alpha^{-/-}$ MPMEC with lysophosphatidylcholine or lysophosphatidic acid alone did not substantially increase the number of Ki-67–positive cells. However, the number of Ki-67–positive cells (expressed as a percentage of that in untreated $cPLA_2\alpha^{+/+}$ MPMEC) was statistically significantly higher in $cPLA_2\alpha^{-/-}$ MPMEC treated with the combination of lysophosphatidylcholine and lysophosphatidic acid compared with untreated $cPLA_2\alpha^{-/-}$ MPMEC (treated vs control: 75% vs 41.4%, difference = 33.6%, 95% CI = 18.3% to 49.7%, $P = .011$) (Figure 1, A). Treatment of $cPLA_2\alpha^{-/-}$ MPMEC with exogenous arachidonic acid, alone, or in combination with lysophosphatidylcholine contributed little to Ki-67 immunofluorescence (Figure 1, A). This latter combination—lysophosphatidylcholine plus arachidonic acid—served as a negative control for the observed effect of lysophosphatidylcholine plus lysophosphatidic acid because it accounted for the potential effects of the addition of ethanol (the diluent) and lipid contaminents in ethanol. Treatment of 3B-11 cells with CDIBA and lysophosphatidylcholine or lysophosphatidic acid resulted in slight increases in the number of Ki-67–positive cells compared with cells treated with CDIBA alone (56% vs 44% and 58% vs 44%, respectively; Figure 1, B). Treatment of 3B-11 cells with CDIBA and arachidonic acid also resulted in a slight increase in the number of Ki-67–positive cells compared with cells treated with CDIBA alone (56% vs 44%; Figure 1, B). Combined treatment with lysophosphatidylcholine and arachidonic acid further increased the number of Ki-67–positive cells to 62% (Figure 1, B). However, only 3B-11 cells treated with CDIBA and the combination of lysophosphatidylcholine and lysophosphatidic acid had a statistically significant increase in the number of Ki-67–positive cells compared with 3B-11 cells treated with CDIBA alone (CDIBA+ lysophosphatidylcholine + lysophosphatidic acid vs CDIBA: 81% vs 44%, difference = 37%, 95% CI = 34.1% to 41.6%, $P = .001$) (Figure 1, B). Similar results were obtained using the BrdU incorporation assay, in which the addition of exogenous lysophosphatidylcholine and lysophosphatidic acid to CDIBA-treated 3B-11 cells resulted in increased BrdU incorporation compared with cells treated with CDIBA alone (data not shown). Thus, these results indicate that in addition to arachidonic acid, both $cPLA_2$-dependent lysophosphatidylcholine and lysophosphatidic acid may be involved in vascular endothelial cell proliferation.

Effect of Lysophospholipids on Invasion and Migration of $cPLA_2$-Deficient and CDIBA-Treated Vascular Endothelial Cells

Blood vessel formation requires degradation of the extracellular matrix and invasion of adjacent tissues by endothelial cells. Therefore, we next examined the effect of lysophospholipids on endothelial cell invasion and migration. $cPLA_2\alpha^{-/-}$ or $cPLA_2\alpha^{+/+}$ MPMEC or 3B-11 cells were plated onto Matrigel-coated transwell filter inserts and treated for 24 hours with vehicle or with 2 μM CDIBA in absence or presence of 10 μM lysophosphatidylcholine, 10 μM lysophosphatidic acid, or 10 μM arachidonic acid. Cells that had migrated through filters were stained with DAPI and counted with the use of fluorescence microscopy. The mean number of migrated cells per HPF was 78% lower in $cPLA_2\alpha^{-/-}$ MPMEC compared with $cPLA_2\alpha^{+/+}$ MPMEC ($cPLA_2\alpha^{-/-}$ vs $cPLA_2\alpha^{+/+}$: 9.3 vs 46.4 migrated cells per HPF, difference = 37.1 migrated cells per HPF, 95% CI = 17.2 to 57.0 migrated cells per HPF, $P = .004$) (Figure 2, A). Treatment of $cPLA_2\alpha^{-/-}$ MPMEC with lysophosphatidylcholine plus arachidonic acid produced only a slight increase in the mean number of migrated cells compared with untreated $cPLA_2\alpha^{-/-}$ MPMEC, whereas treatment with lysophosphatidylcholine plus lysophosphatidic acid produced a statistically significant increase in the mean number of migrated cells ($cPLA_2\alpha^{-/-}$ MPMEC + lysophosphatidylcholine + lysophosphatidic acid vs untreated $cPLA_2\alpha^{-/-}$ MPMEC: 33.5 vs 9.3 migrated cells per HPF, difference = 23.3 migrated cells per HPF, 95% CI = 3.9 to 42.6 migrated cells per HPF, $P < .001$) (Figure 2, A).

Treatment of 3B-11 cells with CDIBA alone reduced the mean number of migrated cells per HPF by 71% compared with vehicle-treated control cells (CDIBA vs control: 10.3 vs 34.9 migrated cells per HPF, difference = 24.6 migrated cells per HPF, 95% CI = 17.8 to 31.7 migrated cells per HPF, $P < .001$) (Figure 2, B). As expected, treatment of 3B-11 cells with CDIBA and arachidonic acid, a known stimulator of cell migration (38,39), increased the mean number of migrated cells per HPF by 58% compared with cells treated with CDIBA alone (CDIBA + arachidonic acid vs CDIBA: 23.6 vs 10.3 migrated cells per HPF, difference = 13.3 migrated cells per HPF, 95% CI = 11.6 to 15.3 migrated cells per HPF, $P < .001$) (Figure 2, B). We observed a similar increase in the mean number of migrated cells per HPF in 3B-11 cells treated with CDIBA and either lysophosphatidylcholine or lysophosphatidic acid compared with 3B-11 cells treated with CDIBA alone (24 [CDIBA + lysophosphatidylcholine] or 21.1 [CDIBA + lysophosphatidic acid] vs 10.3 [CDIBA] migrated cells per HPF, respectively; Figure 2, B). However, compared with 3B-11 cells treated with CDIBA alone, the most pronounced increase in the number of migrated cells was for 3B-11 cells that were treated with CDIBA and either lysophosphatidylcholine plus lysophosphatidic acid (CDIBA + lysophosphatidylcholine + lysophosphatidic acid vs

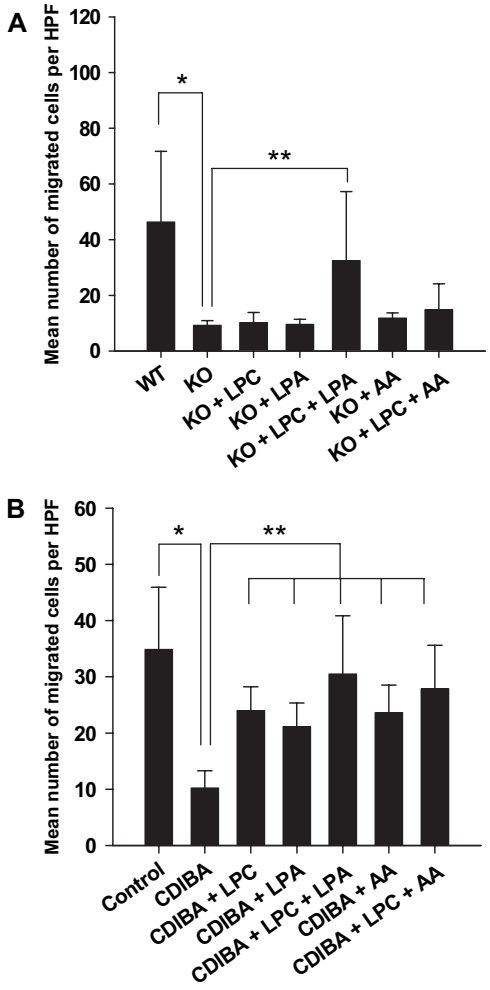

Figure 2. Effects of lysophospholipids on invasion and migration of $cPLA_2$-deficient and CDIBA-treated vascular endothelial cells. $cPLA_2\alpha^{+/+}$ (wild type [WT]) and $cPLA_2\alpha^{-/-}$ (knockout [KO]) murine pulmonary microvascular endothelial cells (**A**) or murine vascular endothelial 3B-11 cells (**B**) were added to the top chambers of 24-well transwell Boyden chamber plates containing 8-μm Matrigel-coated inserts. Fresh medium was added to the bottom chambers; vehicle (control) or 2 μM CDIBA (3B-11 only) was added to the medium in both chambers with or without 10 μM lysophosphatidylcholine (LPC), 10 μM lysophosphatidic acid (LPA), or 10 μM arachidonic acid (AA); and the plates were incubated for 24 hours. The inserts were removed and migrated cells on the lower surfaces of the filters were stained with DAPI (4′,6-diamidino-2-phenylindole) and counted in four randomly chosen high-power microscopic fields (HPFs) per sample. Bar graphs plot the mean number of migrated cells per HPF for triplicate samples from three independent experiments; **error bars** correspond to 95% confidence intervals. A): $*P = .004$ (Student *t* test); $**P < .001$ (analysis of variance [ANOVA]). B): $*P < .001$ (Student *t* test); $**P < .001$ (ANOVA). All *P* values are two-sided.

CDIBA: 30.5 vs 10.3 migrated cells per HPF, difference = 20.2 migrated cells per HPF, 95% CI = 14.1 to 26.4 migrated cells per HPF, $P < .001$) or lysophosphatidylcholine plus arachidonic acid (CDIBA + lysophosphatidylcholine + arachidonic acid vs CDIBA: 27.9 vs 10.3 migrated cells per HPF, difference = 17.6 migrated cells per HPF, 95% CI = 13.6 to 21.6 migrated cells per HPF, $P < .001$) (Figure 2, B). Thus, the ability of MPMEC and 3B-11 vascular endothelial cells to invade and migrate may be dependent on lysophospholipids in addition to the well-characterized arachidonic acid pathway.

Differential Effect of $cPLA_2$ Inhibition on Migration of Vascular Endothelial and Tumor Cells

To examine whether CDIBA-mediated $cPLA_2$ inhibition also affects the migratory ability of tumor cells, we performed a scratch assay for cell migration using 3B-11 and LLC cells. The cells were cultured on plates to 70%–80% confluency, and four parallel scratches were created on each plate using a 10-μL pipette tip. The cells were treated with DMSO or CDIBA (2 μM) for 24 hours, and cells that had migrated into the scratched areas were counted. In 3B-11 cells, compared with DMSO, CDIBA produced a statistically significant reduction in the number of migrated cells per HPF (CDIBA vs DMSO: 25.8% vs 100%, difference = 74.2%, 95% CI = 63.2% to 85.1%, $P < .001$) (Figure 3). By contrast, we observed no statistically significant reduction in the migratory ability of lung tumor LLC cells treated with the $cPLA_2$ inhibitor (Figure 3). These data suggest that $cPLA_2$ may be more important for endothelial cell migration than for tumor cell motility.

Effect of $cPLA_2$ Inhibition on Tubule Formation by Vascular Endothelial Cells

One of the initial stages in angiogenesis is the assembly of vascular endothelial cells into tubular vessels. To examine whether $cPLA_2$ plays a role in this process, we performed a capillary-like tubule formation assay. 3B-11 cells and HUVEC were plated onto Matrigel-coated 24-well plates in medium that contained vehicle or CDIBA (2 μM). The cells were incubated at 37°C until tubules formed from control cells (6 hours for 3B-11 and 24 hours for HUVEC). Tubule formation was then analyzed by light microscopy. In 3B-11 cells, treatment with CDIBA reduced tubule formation by 64% compared with vehicle (average number of tubules per HPF, CDIBA vs vehicle: 12 vs 32.6, difference = 20.6, 95% CI = 17.0 to 24.2, $P = .005$) (Figure 4). In HUVEC, treatment with CDIBA reduced tubule formation by 40% compared with vehicle (average number of tubules per HPF, CDIBA vs vehicle: 12.3 vs 20.3, difference = 8.0, 95% CI = 5.8 to 10.3, $P = .009$) (Figure 4). Thus, these results suggest that $cPLA_2$ may play a pivotal role in the formation of a functional vascular network.

Effect of $cPLA_2$ Inhibition on Tumor Growth

We next examined whether $cPLA_2$ inhibition is sufficient to suppress tumor growth in syngeneic heterotopic mouse tumor models of lung cancer (LLC cells) and glioblastoma (GL261 cells). $cPLA_2\alpha^{+/+}$ C57/BL6 mice (n = 6–7 mice per group) received subcutaneous injections of LLC or GL261 tumor cells in the right hind limbs. Tumor-bearing mice were treated intraperitoneally with CDIBA (0.5 or 1.0 mg per kg body weight) or vehicle once daily for five or seven consecutive days. Tumor volume was monitored by external caliper measurements at 48-hour intervals, until tumor volumes reached approximately 700 mm^3. Compared with mice treated with vehicle, LLC tumor growth in mice treated with CDIBA was delayed by 5 days (average number of days to reach tumor volume of 700 mm^3, CDIBA vs vehicle: 16.8 vs 11.8, difference = 5, 95% CI = 3.6 to 6.4, $P = .04$) (Figure 5, A and B). In the GL261 glioma model, the delay in tumor growth was even more pronounced in mice treated with CDIBA compared with mice treated with vehicle. Following treatment cessation, inhibition of tumor growth was sustained from day 7 to day 9. Furthermore, 2 days after

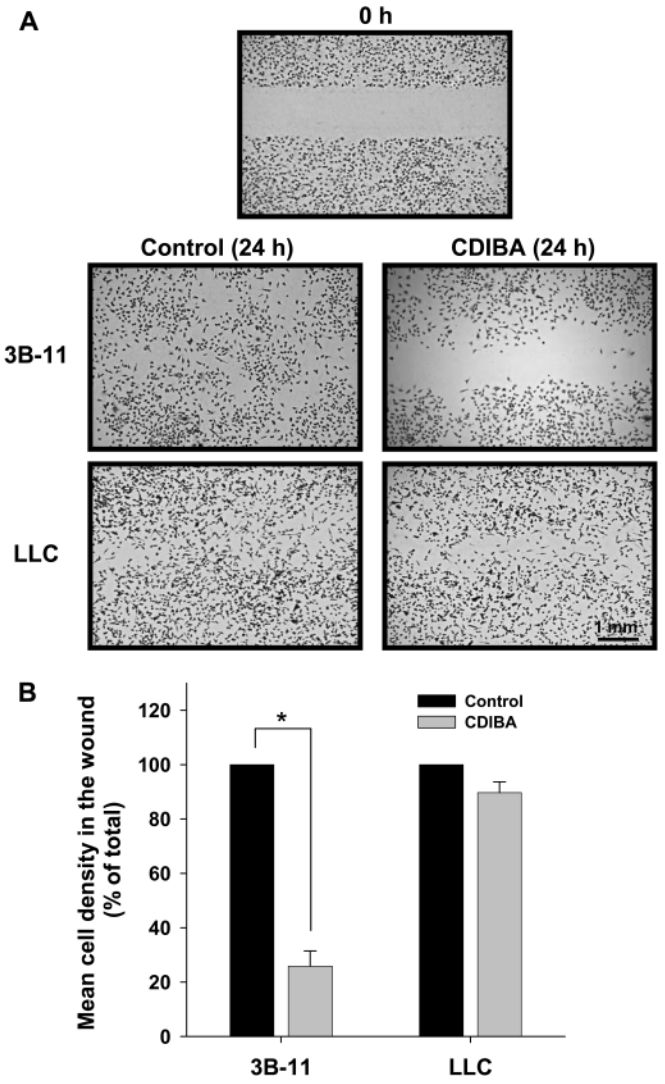

Figure 3. Differential effect of $cPLA_2$ inhibition on migration of vascular endothelial and tumor cells. A scratch assay for cell migration was performed on 3B-11 or Lewis lung carcinoma (LLC) cells grown to 70%–80% confluency. Four parallel wounds were created on each plate using a 10-μL pipette tip, and the cells were treated with dimethyl sulfoxide (control) or the $cPLA_2$ inhibitor CDIBA (2 μM) for 24 hours. The cells were then stained with 1% methylene blue, and cells inside and outside of the wound boundaries were counted. Migration is expressed as mean cell density within the wound. **A**) Representative micrographs of stained cells (at ×10 magnification). **B**) Bar graph of the average cell density within the wound from three independent experiments; **error bars** correspond to 95% confidence intervals. **P* < .001 (two-sided Student *t* test).

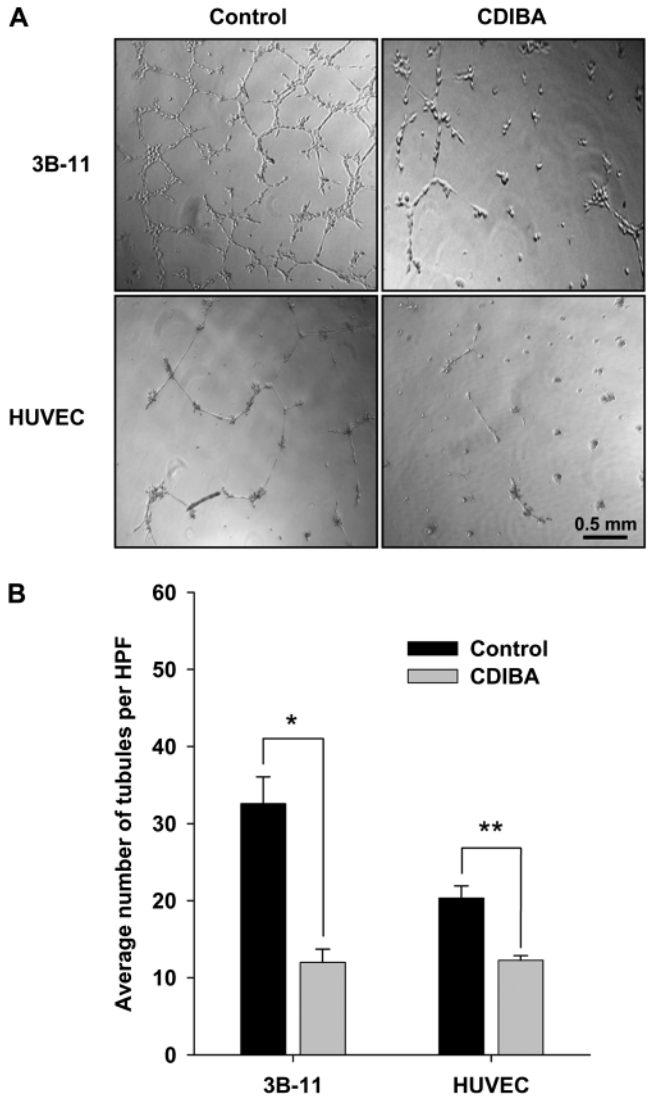

Figure 4. Effect of $cPLA_2$ inhibition on tubule formation by vascular endothelial cells. 3B-11 cells or human umbilical vein endothelial cells (HUVEC) were cultured on Matrigel-coated 24-well plates in the absence (control) or presence of 2 μM CDIBA. Capillary tubule formation was evaluated after 6 (3B-11) or 24 (HUVEC) hours of incubation. Tubule formation was quantified as the number of tubules per high-power microscopic field (HPF) in four randomly selected HPF per sample. **A**) Representative micrographs of treated cells (at ×20 magnification). **B**) Bar graph of the mean number of tubules per HPF for 3B-11 and HUVEC from three independent experiments; **error bars** correspond to 95% confidence intervals. Control vs CDIBA: **P* = .005 and ***P* = .009 (two-sided Student *t* test).

the seventh and final treatment, 50% of CDIBA-treated mice exhibited complete tumor regression, and the regressed tumors remained undetectable throughout the remainder of the study (Figure 5, C). Volume calculations for the remaining tumors revealed that GL261 tumors in CDIBA-treated mice were statistically significantly smaller than those in mice treated with vehicle (mean volume on day 21, CDIBA vs vehicle: 40.1 vs 247.4 mm^3, difference = 207.3 mm^3, 95% CI = 20.9 to 293.7 mm^3, *P* = .021) (Figure 5, D).

To verify that CDIBA inhibited the enzymatic activity of $cPLA_2$ in vivo, we analyzed plasma samples obtained from the previously treated LLC tumor–bearing mice before treatment and immediately after administration of the final treatment with vehicle or CDIBA. In CDIBA-treated mice, $cPLA_2$ activity was reduced by 59% after the final treatment compared with $cPLA_2$ activity before treatment initation (1.4 vs 4.3 μmol/min/mL, difference = 2.9 μmol/min/mL, 95% CI = 2.5 to 3.3 μmol/min/mL, *P* = .004). By contrast, in mice treated with vehicle alone, a statistically significant decrease in plasma $cPLA_2$ activity was not observed after treatment (Figure 5, E). Plasma lysophosphatidic acid levels were also measured before treatment and immediately after the final treatment. There was no statistically significant difference in plasma lysophosphatidic acid concentration following treatment with CDIBA as compared with plasma samples obtained before the

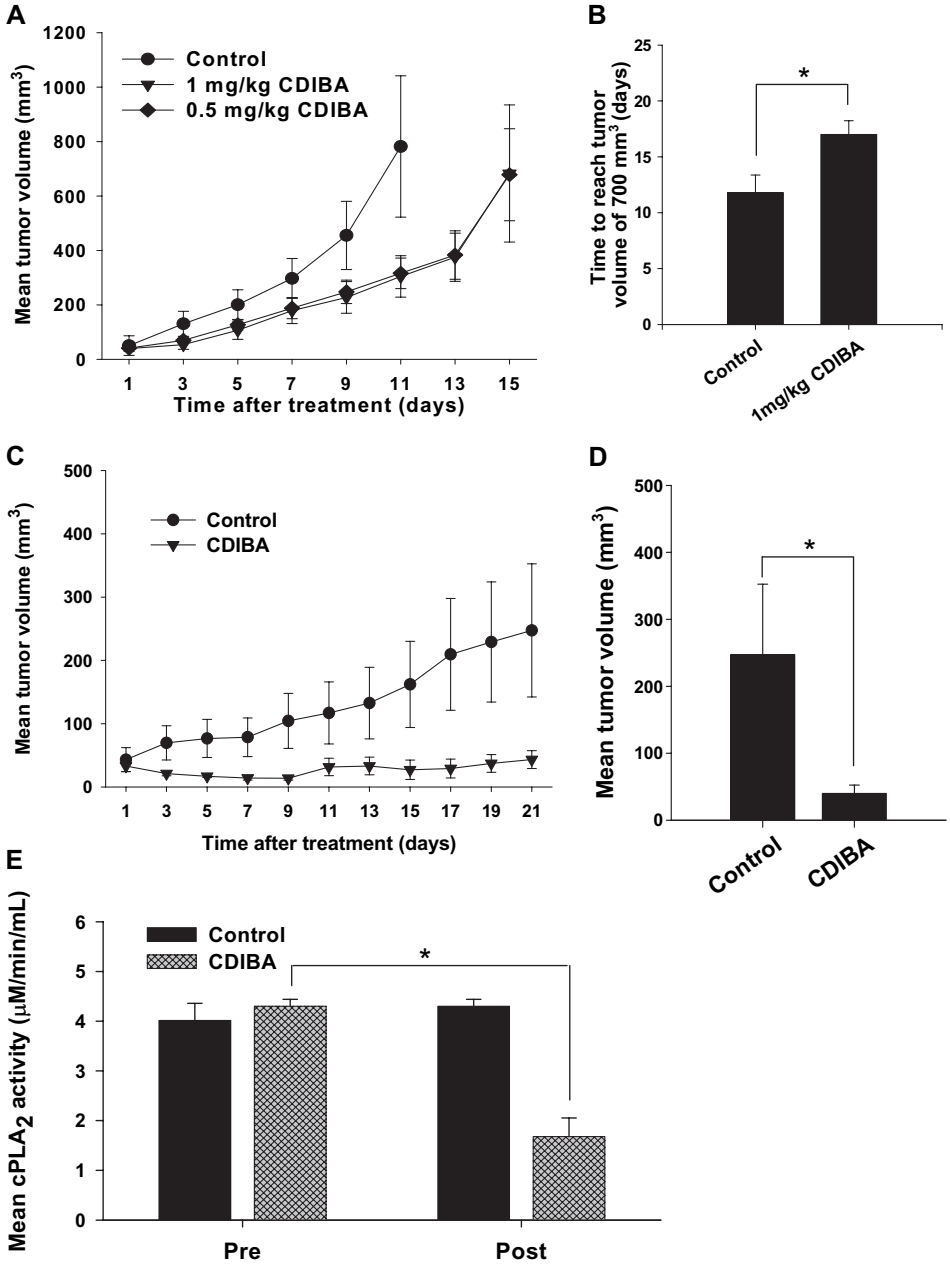

Figure 5. Effect of $cPLA_2$ inhibition on tumor growth. Lewis lung carcinoma (LLC) (**A** and **B**) or GL261 cells (**C** and **D**) were injected subcutaneously into the hind limbs of $cPLA_2\alpha^{+/+}$ C57/BL6 mice. To inhibit $cPLA_2$ in vivo, approximately 2 weeks after tumor cell injection, mice received intraperitoneal injections of vehicle (control) or CDIBA at 0.5 or 1.0 mg per kg body weight once per day for five (LLC) or seven (GL261) consecutive days (n = 6–7 mice per group). $cPLA_2$ activity was measured by an enzymatic activity assay in plasma obtained from LLC tumor–bearing mice before treatment initiation and immediately after the final treatment. Tumor volume was measured using an external caliper. **A**) Mean LLC tumor volume; treatment administered on days 1–5. **B**) Mean number of days for LLC tumors to reach 700 mm^3 in mice treated with vehicle and in mice treated with 1.0 mg CDIBA per kg body weight. *P = .04 (Student t test). **C**) Mean GL261 tumor volume; treatment administered on days 1–7. Control vs CIBDA: P = .03 (day 9), P = .03 (day 13), P = .01 (day 15), P = .01 (day 17), P = .02 (day 19), and P = .02 (day 21) (longitudinal analysis of least squares means). **D**) Mean GL261 tumor volume for each treatment group on day 21. *P = .021 (Student t test). **E**) $cPLA_2$ activity in plasma from control and CDIBA-treated mice before treatment initiation (pre) and immediately after the final treatment (post). *P = .004 (analysis of variance). **Error bars** correspond to 95% confidence intervals, and all P values are two-sided.

initiation of treatment (data not shown). Thus, treatment with CDIBA in vivo inhibited the enzymatic activity of $cPLA_2$ but did not affect the circulating plasma levels of lysophosphatidic acid.

Tumor Growth in $cPLA_2\alpha$-Deficient Mice

To further examine the role of $cPLA_2$ in angiogenesis and tumor progression, we monitored the growth of tumors in $cPLA_2\alpha^{+/+}$ and $cPLA_2\alpha^{-/-}$ mice that were injected subcutaneously into the hind limb with LLC cells or GL261 cells (n = 6–7 mice per group). Tumor volumes were monitored at 48-hour intervals using power Doppler sonography until they exceeded a volume of 700 mm^3 or a diameter of 15 mm. Despite an initial tumor take rate of 100% and progression to tumor volumes in the range of 100–200 mm^3 by 14 days after tumor cell injection in both groups of mice, complete

spontaneous LLC tumor regression was observed in 50% of the $cPLA_2\alpha^{-/-}$ mice but in none of the $cPLA_2\alpha^{+/+}$ mice. Furthermore, tumor volume measurements from day 16 onward revealed a statistically significant reduction in mean tumor volume in the remaining tumors from $cPLA_2\alpha^{-/-}$ mice compared with tumors from $cPLA_2\alpha^{+/+}$ mice (mean tumor volume on day 16, $cPLA_2\alpha^{-/-}$ vs $cPLA_2\alpha^{+/+}$: 90 vs 518.3 mm^3, difference = 428.3 mm^3, 95% CI = 223.1 to 633.5 mm^3, $P = .047$) (Figure 6, A). The effects of $cPLA_2$ deficiency on tumor growth were even more pronounced in the GL261 tumor model (Figure 6, B). Whereas $cPLA_2\alpha^{+/+}$ mice exhibited gradual tumor growth progression (tumor take = 100%), GL261 tumor formation in $cPLA_2\alpha^{-/-}$ mice remained undetectable 1 month after the injection of tumor cells (tumor take = 0%).

Vascularity, Pericyte Coverage, and Necrosis in LLC Tumors From $cPLA_2\alpha^{-/-}$ Mice

To determine the effects of $cPLA_2$ deficiency on tumor vascularity, LLC tumors from $cPLA_2\alpha^{+/+}$ and $cPLA_2\alpha^{-/-}$ mice were resected once tumors reached volumes of 700 mm^3, formalin fixed, and sectioned, and the sections were examined for microvessel density by immunohistochemical staining with an antibody against vWF, a known vascular endothelial cell marker (Figure 7, A). Immunohistochemical examination revealed that tumors from $cPLA_2\alpha^{-/-}$ mice had statistically significant fewer vessels per HPF compared with tumors from wild-type mice (mean number of vessels per HPF, $cPLA_2\alpha^{-/-}$ vs $cPLA_2\alpha^{+/+}$: 2.4 vs 5.4, difference = 3.0 vessels per HPF, 95% CI = 2.7 to 3.2 vessels per HPF, $P < .001$) (Figure 7, A and B). Hematoxylin–eosin staining of tumor sections revealed multiple necrotic areas in tumors from $cPLA_2\alpha^{-/-}$ mice, but only minimal necrosis in tumors from $cPLA_2\alpha^{+/+}$ mice,

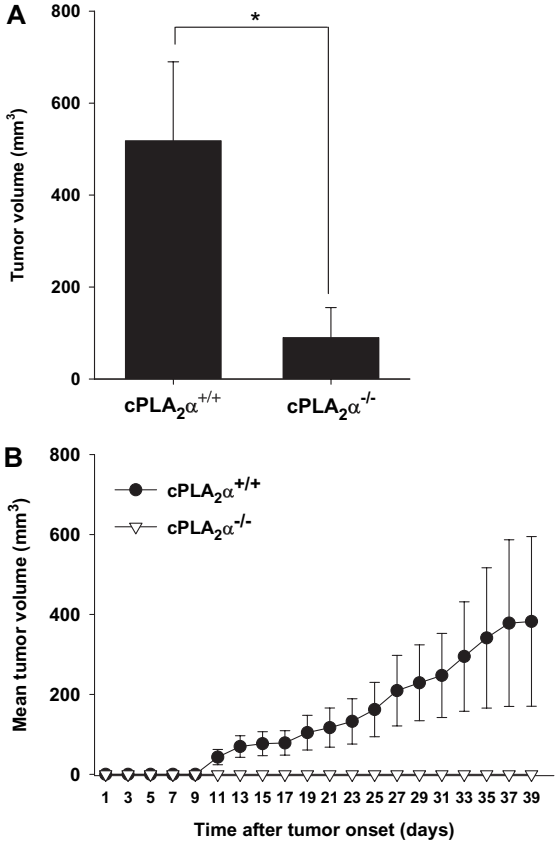

Figure 6. Tumor growth in $cPLA_2\alpha$-deficient mice. Lewis lung carcinoma (LLC) or GL261 cells were injected subcutaneously into the hind limbs of $cPLA_2\alpha^{+/+}$ or $cPLA_2\alpha^{-/-}$ C57/BL6 mice (n = 6–7 mice per group). Tumor volume was measured using power Doppler sonography at 48-hour intervals beginning 1 week after injection and ending when tumors reached a volume of 700 mm^3 or a diameter of 15 mm). **A**) Mean LLC tumor volume for $cPLA_2\alpha^{+/+}$ mice and for remaining tumors from $cPLA_2\alpha^{-/-}$ mice at day 16 after tumor cell injection. $*P = .047$ (two-sided Student *t* test). **B**) Mean GL261 tumor volumes. $cPLA_2\alpha^{+/+}$ vs $cPLA_2\alpha^{-/-}$. Days 11–39: $P < .001$ (longitudinal analysis of least squares means). **Error bars** correspond to 95% confidence intervals.

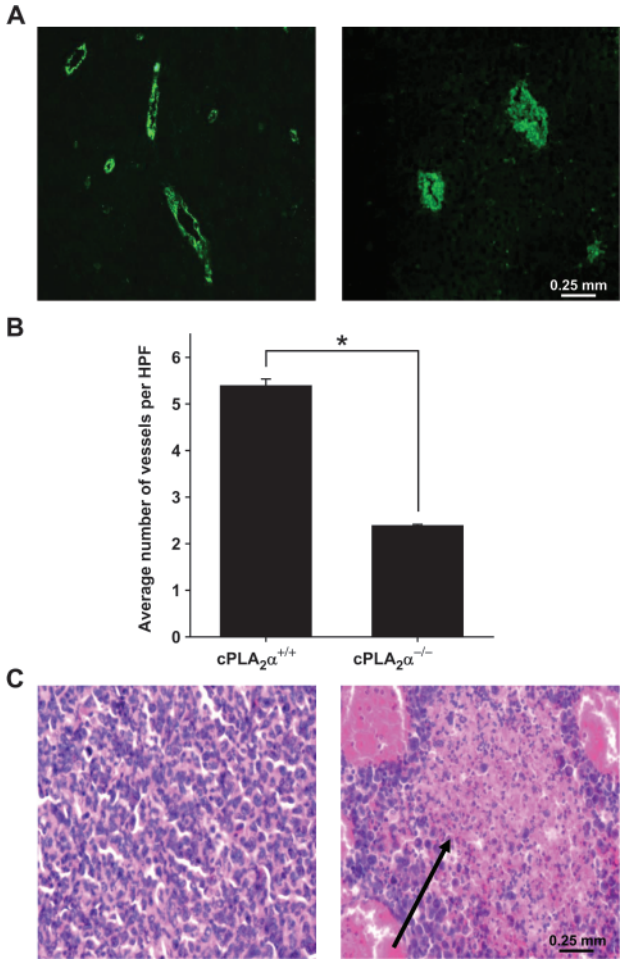

Figure 7. Vascularity and necrosis in tumors from $cPLA_2\alpha^{-/-}$ mice. Lewis lung carcinoma (LLC) cells were injected subcutaneously into the hind limbs of $cPLA_2\alpha^{+/+}$ and $cPLA_2\alpha^{-/-}$ mice (n = 6–7 mice per group). Once the average tumor volume reached approximately 700 mm^3, the mice were killed by cervical dislocation and their tumors were resected and fixed in 10% formalin. Fixed tumors were then sectioned, and the sections were stained with an antibody against von Willebrand factor (vWF) (an endothelial cell marker) or hematoxylin–eosin. vWF-positive vessels were counted with the use of immunofluorescence microscopy. **A**) Representative micrographs of positive anti-vWF staining (**green**) at ×40 magnification in sections of tumors from $cPLA_2\alpha^{+/+}$ (**left**) and $cPLA_2\alpha^{-/-}$ (**right**) mice. **B**) Mean number of tumor blood vessels per high-power microscopic field (HPF) from $cPLA_2\alpha^{+/+}$ and $cPLA_2\alpha^{-/-}$ mice (three mice per group; six HPFs per slide). **Error bars** correspond to 95% confidence intervals. $*P < .001$ (two-sided Student *t* test). **C**) Representative micrographs of hematoxylin–eosin-stained sections of LLC tumors from $cPLA_2\alpha^{+/+}$ (**left**) and $cPLA_2\alpha^{-/-}$ (**right**) mice (at ×40 magnification). **Black arrow** indicates necrosis.

suggesting that $cPLA_2$ may be an important factor for tumor formation, growth, and maintenance (Figure 7, C).

To investigate whether $cPLA_2$ is involved in tumor blood vessel maturation, LLC tumor sections were co-stained with antibodies to vWF and α-SMA or desmin. As two proteins that are expressed by pericytes (cells that surround small blood vessels), α-SMA and desmin are often used to identify the stage of vascular development (40). Microscopic assessment of α-SMA immunofluorescence revealed substantial pericyte coverage of the tumor vasculature in LLC tumors from $cPLA_2\alpha^{+/+}$ mice, whereas in tumors from $cPLA_2\alpha^{-/-}$ mice, vessel-encircling pericytes were undetectable (Figure 8, A). Because α-SMA expression may depend on the stage of pericyte maturation (40), we also stained tumor sections with an antibody against desmin, which is expressed by mature and immature pericytes (40). Although desmin was detected in tumor vasculature from $cPLA_2\alpha^{+/+}$ mice, no desmin-positive cells were observed within tumor blood vessels from $cPLA_2\alpha^{-/-}$ mice (Figure 8, B). These marked differences in desmin and α-SMA staining suggest that, in addition to its role in endothelial cell function, $cPLA_2$ may also be required for pericyte recruitment and vessel maturation.

Discussion

Whereas previous studies have shown that $cPLA_2$ and arachidonic acid are associated with tumor progression, this study provides evidence that $cPLA_2$ promotes tumor angiogenesis through a lysophospholipid-mediated mechanism. Our data from cell culture experiments implicate key regulatory roles for $cPLA_2$ and the lysophospholipids lysophosphatidylcholine and lysophosphatidic acid in proliferation and invasive migration of and tubule formation by vascular endothelial cells. In addition, we showed in a mouse tumor model that, despite expression of $cPLA_2$ in the tumor cells, $cPLA_2$ deficiency within the host component resulted in delayed tumor growth, impaired tumor vascularization, and decreased

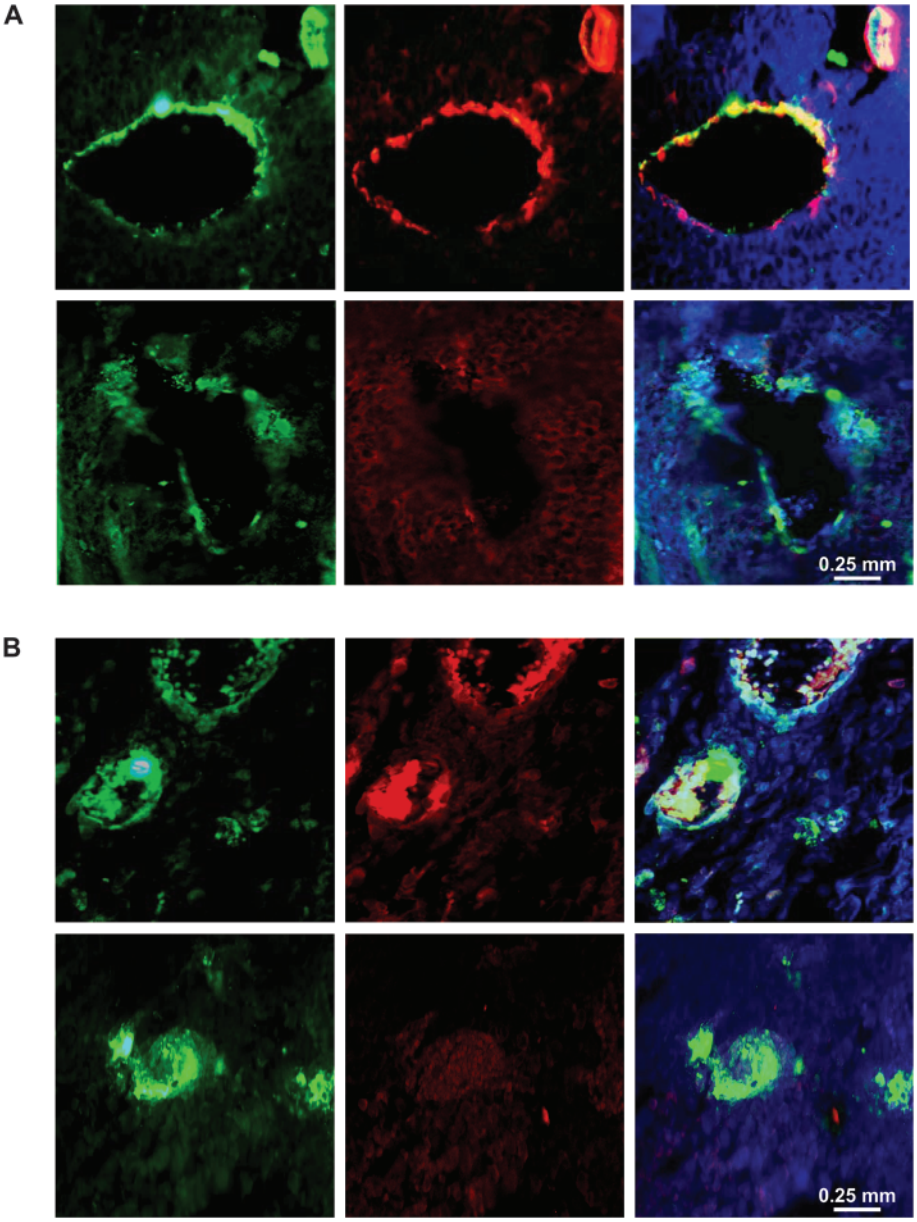

Figure 8. Pericyte coverage of blood vessels in tumors from $cPLA_2\alpha^{+/+}$ and $cPLA_2\alpha^{-/-}$ mice. Formalin-fixed Lewis lung carcinoma (LLC) tumors from $cPLA_2\alpha^{+/+}$ (**upper rows**) and $cPLA_2\alpha^{-/-}$ (**lower rows**) mice were sectioned and co-stained with antibodies against von Willebrand factor (**left panels**) and either α-smooth muscle actin (**middle panels, A**) or desmin (**middle panels, B**) and counterstained with DAPI (4′,6-diamidino-2-phenylindole). **A**) Representative micrographs of immunofluorescence staining for von Willebrand factor (**green**), α-smooth muscle actin (**red**), and DAPI (**blue**) in tumors from $cPLA_2\alpha^{+/+}$ and $cPLA_2\alpha^{-/-}$ mice (at ×40 magnification). **Right panels** present merged immunofluorescence staining of von Willebrand factor and cells positive for α–smooth muscle actin (**yellow**). **B**) Representative micrographs of immunofluorescence staining for von Willebrand factor (**green**), desmin (**red**), and DAPI (**blue**) in tumors from $cPLA_2\alpha^{+/+}$ and $cPLA_2\alpha^{-/-}$ mice (at ×40 magnification). **Right panels** present merged immunofluorescence staining of von Willebrand factor and cells positive for desmin (**yellow**).

pericyte development in tumor blood vessels. Thus, these clinically relevant findings identify $cPLA_2$ and lysophospholipids as important molecular targets for angiogenic blockade and anticancer therapy.

Blood vessel formation is a fundamental process that occurs during both normal and pathological tissue growth. In malignancies such as lung cancer and glioblastoma, vascularization is often excessive and associated with tumor progression (41). Multiple antiangiogenic agents have been developed in an effort to inhibit tumor growth. However, although several angiogenesis inhibitors have produced an enhanced clinical benefit, many of these pharmacological agents result in only transitory improvements that are followed by increased tumor resistance (42). Thus, the development of novel effective antiangiogenic therapies could improve tumor control in treatment-resistant vascularized cancers, such as lung carcinoma and glioblastoma. In this study, we identify a key regulatory role for $cPLA_2$ in tumor angiogenesis and provide evidence that inhibition of $cPLA_2$ activity may prevent the formation of a functional tumor vascular network.

We found that $cPLA_2$ inhibition with CDIBA provided a statistically significant attenuation of capillary-like tubule formation in vitro in two vascular endothelial cell lines (3B-11 and HUVEC). In addition, results from a scratch assay revealed that treatment of the endothelial cell lines with CDIBA reduced cell migration by 75% but had no statistically significant effect on migration of lung tumor cells. Thus, these data suggest that $cPLA_2$ contributes to both the formation of tubules and the migratory ability of vascular endothelial cells during tumor vascularization.

The migration and tubule formation ability of vascular endothelial cells depend on the ability of the vascular endothelium to degrade both the basement membrane and the extracellular matrix of the surrounding connective tissue (41). In a transwell filter assay, we found that $cPLA_2$ inhibition dramatically reduced the ability of cultured vascular endothelial cells to degrade a basement membrane matrix (ie, solidified Matrigel) and migrate through a Matrigel-coated filter. These results suggest that $cPLA_2$ has an essential role in the migratory function of vascular endothelial cells. Because $cPLA_2$ is responsible for the production of the bioactive lipid mediators lysophosphatidylcholine, arachidonic acid, and lysophosphatidic acid, we examined which of these products contributes to vascular endothelial cell migration. Although addition of lysophosphatidylcholine, lysophosphatidic acid, or arachidonic acid alone to the culture medium resulted in increased migration of $cPLA_2\alpha^{-/-}$ MPMEC and 3B-11 cells treated with CDIBA, the most pronounced effect was observed with the addition of lysophosphatidylcholine plus lysophosphatidic acid or lysophosphatidylcholine plus arachidonic acid. These results indicate that, although arachidonic acid and lysophosphatidic acid can regulate endothelial cell migration (25–27,32), the less well characterized lysophosphatidylcholine pathway may also play an important role in this process.

In addition to endothelial cell migration, tumor vascularization requires the proliferation of endothelial cell populations. To examine the effects of CDIBA on cell proliferation, we assessed staining with an antibody against Ki-67, a well-known marker of proliferation (43,44), in MPMEC, 3B-11, and LLC cells. The number of Ki-67–positive cells was statistically significantly lower in MPMEC from $cPLA_2\alpha^{-/-}$ mice compared with MPMEC from $cPLA_2\alpha^{+/+}$ mice and in 3B-11 cells treated with CDIBA compared with 3B-11 cells treated with vehicle. Furthermore, BrdU incorporation but not metabolic activity was also reduced in CDIBA-treated 3B-11 cells compared with vehicle-treated cells, suggesting that $cPLA_2$ inhibition affects proliferation rather than cell viability. LLC tumor cell proliferation, however, remained unchanged by $cPLA_2$ inhibition. The addition of lysophosphatidylcholine plus arachidonic acid to the culture medium resulted in a modest increase in Ki-67 staining, whereas the greatest increase was observed in endothelial cells treated with lysophosphatidylcholine plus lysophosphatidic acid. These findings were further supported by evidence from primary cultures of MPMEC, in which the most pronounced increase in cell proliferation was observed in $cPLA_2\alpha^{-/-}$ MPMEC treated with the combination of lysophosphatidylcholine and lysophosphatidic acid. These data demonstrate a key role for $cPLA_2$ in endothelial cell proliferation and indicate that two lysophospholipids—lysophosphatidylcholine and lysophosphatidic acid—may act as effectors for this stage of angiogenesis.

To examine the role of $cPLA_2$ in tumor growth, we studied mouse tumor models of lung carcinoma and glioblastoma. We found that intraperitoneal injection of CDIBA, a chemical inhibitor of $cPLA_2$, into tumor-bearing mice provided a statistically significant delay in tumor growth in both tumor models. In addition, in the glioblastoma model, we observed tumor regression while the mice were receiving CDIBA. Given the high level of vascularity in glioblastoma multiforme tumors, this unexpected biological response may be because of impaired blood flow, which may have ultimately prevented cancer growth (45–49). Moreover, GL261 tumor growth suppression was sustained for several days after the cessation of treatment, suggesting that CDIBA exhibits a prolonged pharmacodynamic effect. Analysis of plasma samples from LLC tumor–bearing mice revealed a statistically significant reduction in $cPLA_2$ activity in CDIBA-treated mice compared with vehicle-treated mice, confirming previous reports of CDIBA-dependent inhibition of $cPLA_2$ activity in vivo (36,50–53). However, there was no substantial change in plasma lysophosphatidic acid concentration. These results indicate that $cPLA_2$ inhibition may have a transient effect on lysophosphatidylcholine production, but no effect on the circulating plasma levels of lysophosphatidic acid. Because lysophosphatidic acid can also be generated independently of lysophosphatidylcholine by a variety of other enzymes, including phospholipase D, phospholipase A1, and secretory phospholipase A2, reduced lysophosphatidylcholine levels do not necessarily correlate with decreased lysophosphatidic acid production (28,54).

Our findings in the mouse models support previous studies that showed decreased tumorigenesis in mice genetically deficient in $cPLA_2$ (55,56). In the more recent of these studies (56), $cPLA_2\alpha^{-/-}$ mice exhibited decreased lung tumor metastasis as a result of reduced production of interleukin 6 by the tumors and a decrease in the number of macrophages surrounding the tumor. However, neither study considered whether tumor blood vessel formation was involved in the impairment of tumorigenesis. In this study, we analyzed the role of $cPLA_2$ in tumor vascularization in $cPLA_2\alpha^{+/+}$ and $cPLA_2\alpha^{-/-}$ mice. In the syngeneic heterotopic lung tumor model, we observed that tumor volume in $cPLA_2\alpha^{-/-}$ mice was statistically significantly lesser than that in $cPLA_2\alpha^{+/+}$ mice.

Furthermore, we observed spontaneous lung tumor regression in 50% of the $cPLA_2\alpha^{-/-}$ mice but no such regression in the wild-type mice. Upon histological examination of the remaining tumors, we observed a stastically significant reduction in the number of blood vessels in tumors from $cPLA_2\alpha^{-/-}$ mice compared with tumors from $cPLA_2\alpha^{+/+}$ mice. Furthermore, immunofluorescence staining revealed a striking absence of α-SMA- and desmin-positive pericytes within the tumor vasculature of $cPLA_2\alpha^{-/-}$ mice. Because previous studies have shown that tumor pericytes can regulate vessel integrity, maintenance, and function (40,57–60), the lack of desmin and α-SMA staining in the tumor vasculature of $cPLA_2\alpha^{-/-}$ mice may indicate that $cPLA_2$ is also involved in pericyte recruitment and tumor vessel maturation. In addition, multiple areas of necrosis were present in tumors from $cPLA_2\alpha^{-/-}$ mice, but only minimal necrosis was detected in lung tumors from $cPLA_2\alpha^{+/+}$ mice, suggesting that $cPLA_2$ may be necessary for sufficient tumor blood flow.

We observed an even greater suppression of tumor growth in the glioblastoma tumor model than in the LLC tumor model. Following injection of GL261 tumor cells, gradual tumor progression occurred in $cPLA_2\alpha^{+/+}$ mice, whereas tumor formation in $cPLA_2\alpha^{-/-}$ mice remained undetectable up to 1 month after injection. These results suggest that the presence of $cPLA_2$ activity within the tumor microenvironment contributes to efficient tumor development.

Although these results implicate a novel role for $cPLA_2$ in tumor angiogenesis, this study is not without limitations. First, we used heterotopic model systems to study the effect of $cPLA_2$ on tumor growth. Many studies have shown that the growth advantages of the subcutaneous microenvironment may differ from that of the original tumor organ site (61,62). Moreover, in the case of spontaneous tumor metastasis, orthotopic injection is often necessary to sufficiently represent clinical cancer (61). When assessing tumor growth and angiogenesis in the absence of metastasis, however, subcutaneous model systems are routinely used (63–65). Thus, based on work conducted in previous investigations, and to reduce the morbidity that is associated with orthotopic models of lung cancer and glioblastoma (66), we selected heterotopic tumor models for our study.

A second experimental challenge was revealed during the immunohistochemical examination of pericyte coverage. Because of the diverse functions, locations, and maturation stages of pericytes within various organs, no universal molecular marker of these cells has yet to our knowledge been discovered (40). To address this limitation, we used two different markers—α-SMA and desmin—to identify both mature and immature pericytes. However, we acknowledge that some perivascular cells may not have been recognized by the antibodies to α-SMA and desmin because of tissue specificity or the angiogenic stage of the tumor vasculature.

Together, our findings indicate that $cPLA_2$ and lysophospholipids have a key role in the invasive migration, proliferation, and capillary-like tubule formation of vascular endothelial cells. In addition, we found that in mouse tumor models, $cPLA_2$ deficiency within the host component resulted in delayed tumor growth and impaired tumor vascularization. Thus, these data identify $cPLA_2$ as an important factor in tumor angiogenesis and suggest that $cPLA_2$ may be a novel molecular target for antiangiogenesis cancer therapy.

References

1. Clamon G, Herndon J, Cooper R, Chang AY, Rosenman J, Green MR. Radiosensitization with carboplatin for patients with unresectable stage III non-small-cell lung cancer: a phase III trial of the Cancer and Leukemia Group B and the Eastern Cooperative Oncology Group. *J Clin Oncol.* 1999;17(1):4–11.
2. DeAngelis LM. Brain tumors. *N Engl J Med.* 2001;344(2):114–123.
3. Lee JH, Machtay M, Kaiser LR, et al. Non-small cell lung cancer: prognostic factors in patients treated with surgery and postoperative radiation therapy. *Radiology.* 1999;213(3):845–852.
4. Wagner H Jr. Postoperative adjuvant therapy for patients with resected non-small cell lung cancer: still controversial after all these years. *Chest.* 2000;117(4)(suppl 1):110S–118S.
5. Riely GJ, Miller VA. Vascular endothelial growth factor trap in non small cell lung cancer. *Clin Cancer Res.* 2007;13(15, pt 2):s4623–s4627.
6. Wong ET, Brem S. Taming glioblastoma: targeting angiogenesis. *J Clin Oncol.* 2007;25(30):4705–4706.
7. Suh JH, Barnett GH. Brachytherapy for brain tumor. *Hematol Oncol Clin North Am.* 1999;13(3:635–650, viii–ix.
8. Videtic GM, Gaspar LE, Zamorano L, et al. Use of the RTOG recursive partitioning analysis to validate the benefit of iodine-125 implants in the primary treatment of malignant gliomas. *Int J Radiat Oncol Biol Phys.* 1999;45(3):687–692.
9. Brock MV, Hooker CM, Ota-Machida E, et al. DNA methylation markers and early recurrence in stage I lung cancer. *N Engl J Med.* 2008; 358(11):1118–1128.
10. Hoffman PC, Mauer AM, Vokes EE. Lung cancer. *Lancet.* 2000; 355(9202):479–485.
11. Martini N, Bains MS, Burt ME, et al. Incidence of local recurrence and second primary tumors in resected stage I lung cancer. *J Thorac Cardiovasc Surg.* 1995;109(1):120–129.
12. Mountain CF. Revisions in the International System for Staging Lung Cancer. *Chest.* 1997;111(6):1710–1717.
13. Amir E, Hughes S, Blackhall F, et al. Targeting blood vessels for the treatment of non-small cell lung cancer. *Curr Cancer Drug Targets.* 2008; 8(5):392–403.
14. Levy AP, Levy NS, Wegner S, Goldberg MA. Transcriptional regulation of the rat vascular endothelial growth factor gene by hypoxia. *J Biol Chem.* 1995;270(22):13333–13340.
15. Shweiki D, Neeman M, Itin A, Keshet E. Induction of vascular endothelial growth factor expression by hypoxia and by glucose deficiency in multicell spheroids: implications for tumor angiogenesis. *Proc Natl Acad Sci U S A.* 1995;92(3):768–772.
16. Wachsberger P, Burd R, Dicker AP. Tumor response to ionizing radiation combined with antiangiogenesis or vascular targeting agents: exploring mechanisms of interaction. *Clin Cancer Res.* 2003;9(6):1957–1971.
17. Linkous A, Geng L, Lyshchik A, Hallahan DE, Yazlovitskaya EM. Cytosolic phospholipase A2: targeting cancer through the tumor vasculature. *Clin Cancer Res.* 2009;15(5):1635–1644.
18. Yazlovitskaya EM, Linkous AG, Thotala DK, Cuneo KC, Hallahan DE. Cytosolic phospholipase A2 regulates viability of irradiated vascular endothelium. *Cell Death Differ.* 2008;15(10):1641–1653.
19. Clark JD, Lin LL, Kriz RW, et al. A novel arachidonic acid-selective cytosolic PLA2 contains a Ca(2+)-dependent translocation domain with homology to PKC and GAP. *Cell.* 1991;65(6):1043–1051.
20. Hirabayashi T, Shimizu T. Localization and regulation of cytosolic phospholipase A(2). *Biochim Biophys Acta.* 2000;1488(1–2):124–138.
21. Farooqui AA, Ong WY, Horrocks LA. Inhibitors of brain phospholipase A2 activity: their neuropharmacological effects and therapeutic importance for the treatment of neurologic disorders. *Pharmacol Rev.* 2006;58(3):591–620.
22. Grewal S, Herbert SP, Ponnambalam S, Walker JH. Cytosolic phospholipase A2-alpha and cyclooxygenase-2 localize to intracellular membranes of EA.hy.926 endothelial cells that are distinct from the endoplasmic reticulum and the Golgi apparatus. *FEBS J.* 2005;272(5):1278–1290.
23. Herbert SP, Odell AF, Ponnambalam S, Walker JH. The confluence-dependent interaction of cytosolic phospholipase A2-alpha with annexin A1 regulates endothelial cell prostaglandin E2 generation. *J Biol Chem.* 2007;282(47):34468–34478.

24. Nakanishi M, Rosenberg DW. Roles of cPLA2alpha and arachidonic acid in cancer. *Biochim Biophys Acta.* 2006;1761(11):1335–1343.
25. Folkman J. A new link in ovarian cancer angiogenesis: lysophosphatidic acid and vascular endothelial growth factor expression. *J Natl Cancer Inst.* 2001;93(10):734–735.
26. Kishi Y, Okudaira S, Tanaka M, et al. Autotaxin is overexpressed in glioblastoma multiforme and contributes to cell motility of glioblastoma by converting lysophosphatidylcholine to lysophosphatidic acid. *J Biol Chem.* 2006;281(25):17492–17500.
27. Ptaszynska MM, Pendrak ML, Bandle RW, Stracke ML, Roberts DD. Positive feedback between vascular endothelial growth factor-A and autotaxin in ovarian cancer cells. *Mol Cancer Res.* 2008;6(3):352–363.
28. Aoki J, Inoue A, Okudaira S. Two pathways for lysophosphatidic acid production. *Biochim Biophys Acta.* 2008;1781(9):513–518.
29. Aoki J. Mechanisms of lysophosphatidic acid production. *Semin Cell Dev Biol.* 2004;15(5):477–489.
30. Zhang H, Xu X, Gajewiak J, et al. Dual activity lysophosphatidic acid receptor pan-antagonist/autotaxin inhibitor reduces breast cancer cell migration in vitro and causes tumor regression in vivo. *Cancer Res.* 2009; 69(13):5441–5449.
31. Ambesi A, McKeown-Longo PJ. Anastellin, the angiostatic fibronectin peptide, is a selective inhibitor of lysophospholipid signaling. *Mol Cancer Res.* 2009;7(2):255–265.
32. Herbert SP, Odell AF, Ponnambalam S, Walker JH. Activation of cytosolic phospholipase A2-{alpha} as a novel mechanism regulating endothelial cell cycle progression and angiogenesis. *J Biol Chem.* 2009;284(9): 5784–5796.
33. Peyruchaud O. Novel implications for lysophospholipids, lysophosphatidic acid and sphingosine 1-phosphate, as drug targets in cancer. *Anticancer Agents Med Chem.* 2009;9(4):381–391.
34. Murph M, Mills GB. Targeting the lipids LPA and S1P and their signalling pathways to inhibit tumour progression. *Expert Rev Mol Med.* 2007; 9(28):1–18.
35. Fujita Y, Yoshizumi M, Izawa Y, et al. Transactivation of fetal liver kinase-1/kinase-insert domain-containing receptor by lysophosphatidylcholine induces vascular endothelial cell proliferation. *Endocrinology.* 2006; 147(3):1377–1385.
36. McKew JC, Foley MA, Thakker P, et al. Inhibition of cytosolic phospholipase A2alpha: hit to lead optimization. *J Med Chem.* 2006;49(1):135–158.
37. Bonventre JV. The 85-kD cytosolic phospholipase A2 knockout mouse: a new tool for physiology and cell biology. *J Am Soc Nephrol.* 1999;10(2): 404–412.
38. Moes M, Boonstra J, Regan-Klapisz E. Novel role of cPLA(2)alpha in membrane and actin dynamics. *Cell Mol Life Sci.* 2010;67(9):1547–1557.
39. Navarro-Tito N, Soto-Guzman A, Castro-Sanchez L, Martinez-Orozco R, Salazar EP. Oleic acid promotes migration on MDA-MB-231 breast cancer cells through an arachidonic acid-dependent pathway. *Int J Biochem Cell Biol.* 2010;42(2):306–317.
40. Bergers G, Song S. The role of pericytes in blood-vessel formation and maintenance. *Neuro Oncol.* 2005;7(4):452–464.
41. Goodwin AM. In vitro assays of angiogenesis for assessment of angiogenic and anti-angiogenic agents. *Microvasc Res.* 2007;74(2–3):172–183.
42. Bergers G, Hanahan D. Modes of resistance to anti-angiogenic therapy. *Nat Rev Cancer.* 2008;8(8):592–603.
43. Grosse-Wilde A, Voloshanenko O, Bailey SL, et al. TRAIL-R deficiency in mice enhances lymph node metastasis without affecting primary tumor development. *J Clin Invest.* 2008;118(1):100–110.
44. Teplyuk NM, Galindo M, Teplyuk VI, et al. Runx2 regulates G protein-coupled signaling pathways to control growth of osteoblast progenitors. *J Biol Chem.* 2008;283(41):27585–27597.
45. Dewhirst MW, Cao Y, Moeller B. Cycling hypoxia and free radicals regulate angiogenesis and radiotherapy response. *Nat Rev Cancer.* 2008;8(6): 425–437.
46. Folkman J. Tumor angiogenesis: therapeutic implications. *N Engl J Med.* 1971;285(21):1182–1186.
47. de Bouard S, Herlin P, Christensen JG, et al. Antiangiogenic and anti-invasive effects of sunitinib on experimental human glioblastoma. *Neuro Oncol.* 2007;9(4):412–423.
48. Keshet E, Ben-Sasson SA. Anticancer drug targets: approaching angiogenesis. *J Clin Invest.* 1999;104(11):1497–1501.
49. Plate KH, Risau W. Angiogenesis in malignant gliomas. *Glia.* 1995;15(3): 339–347.
50. Graf C, Zemann B, Rovina P, et al. Neutropenia with impaired immune response to *Streptococcus pneumoniae* in ceramide kinase-deficient mice. *J Immunol.* 2008;180(5):3457–3466.
51. Mounier CM, Ghomashchi F, Lindsay MR, et al. Arachidonic acid release from mammalian cells transfected with human groups IIA and X secreted phospholipase A(2) occurs predominantly during the secretory process and with the involvement of cytosolic phospholipase A(2)-alpha. *J Biol Chem.* 2004;279(24):25024–25038.
52. Ni Z, Okeley NM, Smart BP, Gelb MH. Intracellular actions of group IIA secreted phospholipase A2 and group IVA cytosolic phospholipase A2 contribute to arachidonic acid release and prostaglandin production in rat gastric mucosal cells and transfected human embryonic kidney cells. *J Biol Chem.* 2006;281(24):16245–16255.
53. Patel MI, Singh J, Niknami M, et al. Cytosolic phospholipase A2-alpha: a potential therapeutic target for prostate cancer. *Clin Cancer Res.* 2008; 14(24):8070–8079.
54. Gaits F, Fourcade O, Le Balle F, et al. Lysophosphatidic acid as a phospholipid mediator: pathways of synthesis. *FEBS Lett.* 1997;410(1):54–58.
55. Meyer AM, Dwyer-Nield LD, Hurteau GJ, et al. Decreased lung tumorigenesis in mice genetically deficient in cytosolic phospholipase A2. *Carcinogenesis.* 2004;25(8):1517–1524.
56. Weiser-Evans MC, Wang XQ, Amin J, et al. Depletion of cytosolic phospholipase A2 in bone marrow-derived macrophages protects against lung cancer progression and metastasis. *Cancer Res.* 2009;69(5):1733–1738.
57. Gerhardt H, Betsholtz C. Endothelial-pericyte interactions in angiogenesis. *Cell Tissue Res.* 2003;314(1):15–23.
58. Morikawa S, Baluk P, Kaidoh T, Haskell A, Jain RK, McDonald DM. Abnormalities in pericytes on blood vessels and endothelial sprouts in tumors. *Am J Pathol.* 2002;160(3):985–1000.
59. Rucker HK, Wynder HJ, Thomas WE. Cellular mechanisms of CNS pericytes. *Brain Res Bull.* 2000;51(5):363–369.
60. Sennino B, Falcon BL, McCauley D, et al. Sequential loss of tumor vessel pericytes and endothelial cells after inhibition of platelet-derived growth factor B by selective aptamer AX102. *Cancer Res.* 2007;67(15):7358–7367.
61. Fidler IJ, Naito S, Pathak S. Orthotopic implantation is essential for the selection, growth and metastasis of human renal cell cancer in nude mice [corrected]. *Cancer Metastasis Rev.* 1990;9(2):149–165.
62. Hoffman RM. Orthotopic metastatic mouse models for anticancer drug discovery and evaluation: a bridge to the clinic. *Invest New Drugs.* 1999; 17(4):343–359.
63. Benny O, Fainaru O, Adini A, et al. An orally delivered small-molecule formulation with antiangiogenic and anticancer activity. *Nat Biotechnol.* 2008;26(7):799–807.
64. Bix G, Castello R, Burrows M, et al. Endorepellin in vivo: targeting the tumor vasculature and retarding cancer growth and metabolism. *J Natl Cancer Inst.* 2006;98(22):1634–1646.
65. Fainaru O, Hornstein MD, Folkman J. Doxycycline inhibits vascular leakage and prevents ovarian hyperstimulation syndrome in a murine model. *Fertil Steril.* 2009;92(5):1701–1705.
66. Khanna C, Hunter K. Modeling metastasis in vivo. *Carcinogenesis.* 2005;26(3):513–523.

Funding

Elizabeth H. and James S. McDonnell Distinguished Professorship and National Institutes of Health (Washington, DC; R01-140220; R01-CA112385 and R01-CA88076 to D.E.H.); Elsa U. Pardee foundation (Midland, MI) (E.M.Y.).

Notes

The authors declare no competing financial interests. The sponsors had no involvement in the design of the study; the collection, analysis, and interpretation of the data; the writing of the article; or the decision to submit the article for publication.

We appreciate the gift of $cPLA_2\alpha^{-/-}$ and $cPLA_2\alpha^{+/+}$ mice from Dr J. V. Bonventre (Harvard Medical School, Boston, MA). A. G. Linkous designed the research, performed the experiments, analyzed the data, and wrote the article; D. E. Hallahan and E. M. Yazlovitskaya designed the research, analyzed the data, and wrote the article.

Affiliations of authors: Neuro-Oncology Branch, National Institutes of Health, Bethesda, MD (AGL); Division of Nephrology, Department of Medicine, and Vanderbilt-Ingram Cancer Center, Vanderbilt University, Nashville, TN (EMY); Alvin Siteman Cancer Center and Department of Radiation Oncology, Washington University in St Louis, St Louis, MO (DEH).